Poly(vinyl alcohol) and Poly(sodium styrene sulfonate) Compatibility by Differential Scanning Calorimetry, Fourier Transform Infrared and Scanning Electron Microscopy

Chamekh Mbareck,[1] Trong Quang Nguyen,[2] Jean Marc Saiter[2]

[1]*Université de Nouakchott, F.S.T, P. B. 5026, Nouakchott, Mauritanie*
[2]*Laboratoire: P.B.S. FRE 3101 CNRS, Université de Rouen, Mont-Saint-Aignan 76821, France*

Received 25 December 2008; accepted 9 April 2009
DOI 10.1002/app.30598
Published online 2 July 2009 in Wiley InterScience (www.interscience.wiley.com).

ABSTRACT: To prepare ion-exchange membrane from poly(vinyl alcohol) (PVA) and poly (sodium-4-styrene sulfonate) (PSSNa), the polymer compatibility was investigated by means of differential scanning calorimetry, attenuated total reflection Fourier Transform Infrared spectroscopy, and scanning electron microscopy. Using the strong–fragile concept to interpret the differential scanning calorimetric results, we show that the interactions between the segments of both polymers increase with decrease in PVA fraction. Because of these intermolecular interactions, the PVA crystallinity degree decreased with the decrease in PVA fraction, and a single-transition temperature was observed for the polymer blend in the amorphous phase. At the nanoscopic scale, the Fourier Transform Infrared results show that the PVA/PSSNa compatibility is mainly promoted by hydrogen bonds and dipole–ion interactions between PVA and PSSNa segments, whereas at microscopic scale, the morphology obtained by scanning electron microscopy technique shows that PVA and PSSNa form one homogeneous phase. © 2009 Wiley Periodicals, Inc. J Appl Polym Sci 114: 2261–2269, 2009

Key words: polymer compatibility; PVA; strong-fragile concept; infrared; DSC; SEM; PSSNa

INTRODUCTION

Polymer–polymer compatibility continues to attract the interest of many researchers. Blending of polymers with good compatibility is considered to be a very convenient method to meet new requirements in material properties. Among these, the tailored chemical structure is an important one, especially for the membranes whose separation performances are based on the physicochemical affinity with molecular species.

Polymer blends are solid state solutions in which the components can be completely miscible, partially miscible, or nonmiscible. Different criteria were used to evaluate the polymer–polymer miscibility. Because of its simplicity, the blend transparency is one way often used in practice as a first criterion.[1–4] Although opacity of the materials reflects directly a phase separation, transparency is not enough to declare two polymers miscible. Indeed, a blend may be transparent when the segregated phases have small enough size, or when their refraction indexes have similar values.[2]

Correspondence to: C. Mbareck (chamec1@yahoo.fr).

Journal of Applied Polymer Science, Vol. 114, 2261–2269 (2009)

The glass transition temperature (T_g) of the blend is an other criterion. For a nonmiscible system, each component in the blend exhibits its own T_g, whereas for the miscible blend a single T_g is obtained.[2,5] The miscibility of two polymers indicates the existence of crossinteractions between certain groups of the two polymers. From a thermodynamics point of view, the mixing of polymers of high molecular weight engages a small entropic gain. The existence of interactions in the blend system can be proved by spectroscopic methods, among them infrared spectroscopy is convenient, because it allows the identification of interacting groups.[6–8]

In this domain of polymer miscibility, a miscibility of poly(vinyl alcohol) (PVA) can be obtained with a polymer having groups capable of giving rise to sufficiently strong interactions with the hydroxyl groups to inhibit the PVA crystallite formation.[9,10] PVA and poly (sodium-4-styrene sulfonate) (PSSNa) are hydrophilic polymers that can be used as materials for permselective membranes under the form of semi- interpenetrating polymer networks.[11] The compatibility between PVA and a second polymer comes from hydrogen bond interactions.[9,12–16] The PVA hydroxyl groups have both the hydrogen bond acceptor and donor ability,[15–18] so that self-association occurs naturally in PVA materials, leading to

the formation of a crystalline phase,[19–23] Polymers having chemical groups with both the hydrogen bond acceptor and donor powers like poly(acrylic acid) or poly(styrene sulfonic acid) were reported to be compatible with PVA.[9,16] However, it is not evident that the salts of these polyacids are able to inhibit the PVA crystallite formation, as the hydrogen bond acceptors (i.e., the anions) are already involved in electrostatic interactions with the counter ions whose presence is required by the electrical neutrality of the materials.

In the present work, the interactions between PVA and PSSNa were studied by differential scanning calorimetry (DSC) and infrared spectroscopy. This step was useful to control the preparation of tailored homogeneous membrane with semi-interpenetrating polymer network structure. In recent researches,[24–26] many workers revealed the particular interest of these polymers for the preparation of the polymer eletrolyte fuel cells that are considered as a promising asset for the applications of portabe power and electric vehicles.

EXPERIMENTAL

Materials

PVA was supplied by Aldrich chemical company Ltd. (England) and PSSNa by Aldrich. Their molecular weights were, respectively, ca. 124,000 – 186,000 and 70,000 g/mol. The hydrolysis degree of PVA sample was ca. 87–89%. Both samples were used without any further purification.

Films preparation

The polymer blends were prepared by the solution method. Each polymer was dissolved in water (20 g/L) by stirring the mixture at 90°C under reflux for 1 H. The solutions were then cooled at room temperature, purified respectively through 1.2 μm (PVA) and 0.45 μm (PSSNa) Millipore filters type H. A., mixed in defined proportions and finally, they were cast on a glass plate into films. After evaporation of the solvent (3–4 days at room temperature), the films were kept in a dessicator over P_2O_5 for many days. The film thickness was ca. 100 μm. The PVA/PSSNa weight percentages were used to designate the blend composition.

Fourier Transform Infrared spectrum recording

Before its mounting on the attenuated total reflection device for Fourier Transform Infrared (FTIR) measurements, the films were dried in a vacuum oven at 70°C for 12 h. The FTIR spectrometer was a Nicolet AVATAR 360 FTIR equipped with a Ge attenuated total reflection (ATR) crystal. The spectra were recorded at an incident beam angle of 45°. For each sample, the infrared spectrum is the result of 64 scans with a resolution of 4 cm^{-1}.

Differential scanning calorimetry

The DSC measurements were performed with a Perkin Elmer DSC7 calorimeter under a nitrogen atmosphere. The calorimeter was calibrated, at a heating rate of 10°C/min, by using the melting temperature and enthalpy of indium standard. The weight of the dry sample was 10 mg. As the samples absorb water vapor during its handling, correct DSC thermograms are only obtained when water is allowed to escape from the pan in the first scan through holes pierced through the pan cap. Therefore, the samples were heated in the DSC pan under nitrogen stream at 100°C for 10 min then cooled down to 30°C. The DSC scans were next performed from 30 to 220°C at a heating rate of 10°C/min. The mass lost during this first thermal treatment never exceeded 2% w/w and this mass lost was taken into account for the different mass normalization performed to estimate the different value of enthalpy or heat capacity.

The T_g values were determined as the midpoint of the heat capacity endothermic step, whereas the calorimetric melting temperature (T_m) was determined from the maximum point of the melting peak. This melting temperature is not the conventional one, but in regard with the shape of the endothermic signal of melting we found that the conventional onset temperature is difficult to evaluate with the ad-hoc accuracy. The energy required to melt the crystalline phase of 1 g of polymer material (specific melting enthalpy for the sample) was determined from the area of the melting peak. The ratio of the specific melting energy for the studied sample (ΔH_m) to that for the completely crystalline polymer (ΔH^*_m) characterizes the crystallinity of that polymer in the blend sample.

RESULTS AND DISCUSSION

Polymer compatibility and interactions based on DSC data

It is interesting to point out that there was no visible phase separation between PVA and PSSNa, as all the blend materials were very transparent whatever be their composition. The DSC curves obtained for the different compositions are shown in Figure 1. For each curve, an endothermic step, which is a signature of the glass transition, is observed for temperature between 60 and 90°C. For higher temperatures, an endothermic peak of melting occurs on a large

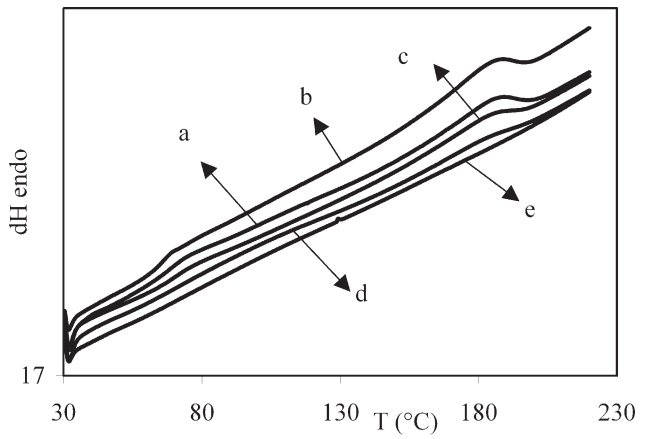

Figure 1 DSC thermograms of PVA/PSSNa: (a) 100/0, (b) 85/15, (c) 70/30, (d) 55/45, and (e) 45/55 blends.

temperature domain between 150 and 210°C excepted for the PVA/PSSNa 45/55, 25/75 and the pure PSSNa samples. An important remark consists to note the lack of exothermic signal for temperatures between the glass transition and the melting transition. This observation allows us to affirm that a crystalline fraction exists in the samples for temperature below the glass transition. Indeed, we have to keep in mind that only the crystalline fraction is able to melt. The determinations of the glass transition temperature and heat capacity difference at T_g, $\Delta Cp_{(T_g)} = Cp_L - Cp_g$ (where the subscripts, L and g, refer to the liquid and the glass states, respectively) are reported in Table I. The quantities ΔH_m and T_m that are the enthalpy of melting and the temperature of melting, respectively, are also given in Table I.

The variations of the glass transition temperature with the fraction of PSSNa are reported in Figure 2. It can be deduced that the change in glass transition temperature $T_g \approx 65$°C for compositions up to 20% of PSSNa is negligible. Variations of T_g are only observed for compositions greater than 20% of PSSNa by an increase of 22°C and a plateau for $T_g \approx$ 85°C seems to be reached for samples with more than 50% of PSSNa. The observation of a unique glass transition temperature suggests a compatibility between the polymers in amorphous phase.[23,27]

The second characteristic of the glass transition is the value of $\Delta Cp_{(T_g)}$. This quantity, which is estimated by Joules per gram of amorphous phase and per Kelvin (J/g K), must be recalculated by taking into account the crystalline fraction that does not participate in the signal at the glass transition. This can be obtained by using the melting peak. Indeed, the melting enthalpy per unit weight of the 100% crystalline PVA (fully crystallized PVA), noted ΔH^*, is 138.6 J/g.[22,28] Thus, the crystalline fraction is obtained by the ratio:

$$X_c = 100(\Delta H_m/\Delta H^*{}_m)$$

By this way, we have estimated the fraction of crystalline phase and the results are also reported in Table I. It was found as shown in Figure 3 that the crystalline fraction varies from 7% for PVA to vanish for compositions greater than 55% of PSSNa. The observed sigmoïd curve shows again that no drastic variations for the values of X_c occur for composition up to 20% of PSSNa. Taking into account these crystalline fractions, the values of $\Delta Cp_{(T_g)}$ have been recalculated by Joules per gram of amorphous phase of total polymer weight (PVA + PSSNa) and per Kelvin. The results are reported in Table I and the variations of this new quantity called $\Delta Cp_{1(T_g)}$ are also shown in Figure 4. In Practical, when compared between the evolutions of $\Delta Cp_{(T_g)}$ and $\Delta Cp_{1(T_g)}$ no drastic difference are found, the value of heat capacity step decreases drastically by increasing the content of PSSNa. As no variations of the glass transition temperature, no drastic variations of the degree of crystallinity are observed for composition up to 20% of PSSNa, we may suppose that the signal obtained at the glass transition concerns a phase made only of PVA. In other words, the value of $\Delta Cp_{(T_g)}$ can be also renormalized in Joules per gram of only amorphous PVA and per Kelvin. The normalization method consists to calculate the real mass of sample that is at the origin of heat capacity ΔCp

TABLE I
Glass Transition Temperature T_g, Heat Capacities at T_g (ΔC_P), Melting Temperature T_m, Melting Enthalpy ΔH_m and Crystallinity Rate of PVA/PSSNa Blends of Different Compositions

W_{PSSNa}	T_g (°C)	ΔCp (J/gK)	T_m (°C)	ΔH_m (J/g)	X_c	ΔCp_1 (J/g K)	ΔCp_2 (J/g K)
0.00	65	0.56	184.5	9.7	7.10	0.60	0.60
0.15	65	0.49	184.0	8.3	7.15	0.53	0.62
0.30	69	0.33	183.0	5.9	6.17	0.35	0.50
0.45	84	0.23	181.0	2.2	2.93	0.24	0.43
0.55	86	0.15	–	0.0	0.00	0.15	0.33
0.75	–	–	–	0.0	0.00	–	–

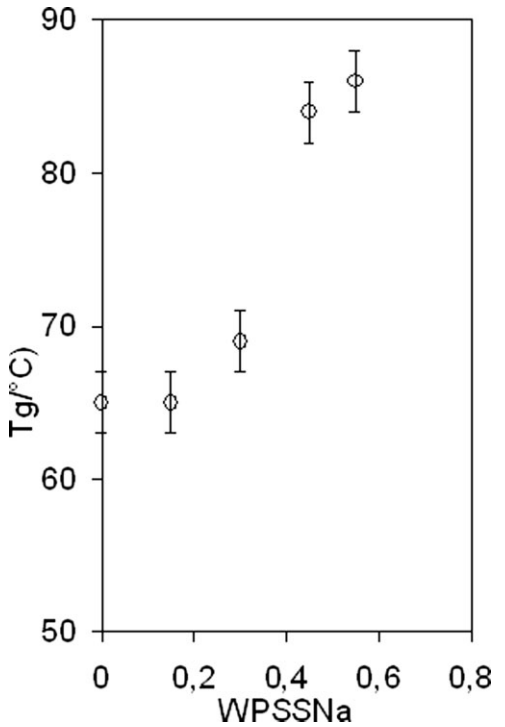

Figure 2 Glass transition temperature of the amorphous phase *versus* PSSNa fraction in PVA/PSSNa blends.

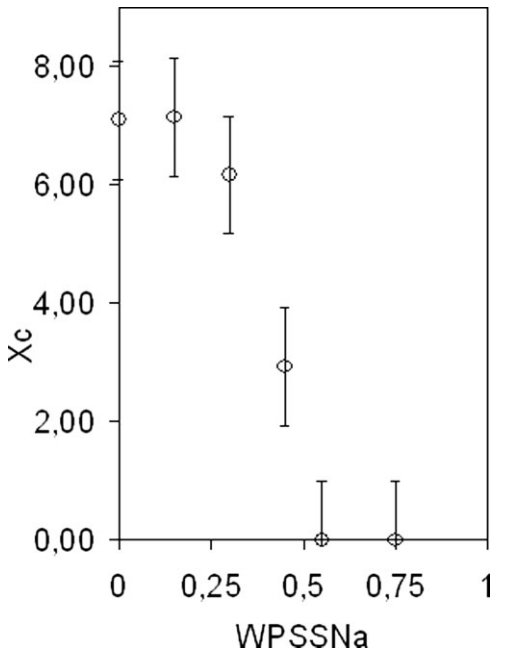

Figure 3 PVA crystallinity vs. PSSNa fraction in PVA/PSSNa blends.

at the glass transition T_g. Of course, the crystalline phase does not participate in determining the value of ΔCp. This calculation leads to the values $\Delta Cp_{2(T_g)}$ reported in Table I and in Figure 4. From this assumption, the variations of heat capacities are now different and upto 20% of PSSNa a constant value is obtained. Thus, the calorimetric data show that for compositions upto 20% of PSSNa, the intermolecular interactions seem to be very weak to overcome the intramolecular interactions between hydroxyl groups along PVA chains. For higher content of PSSNa, strong interactions exist between the polymers leading to a compatibility and an inhibition of the PVA crystallization. The depression of T_m for blends containing one crystallizable components was interpreted by many researchers as a result of intermolecular interactions between miscible polymer.[28–30] For the PVA/PSSNa blends, the slight decrease in T_m of PVA, as given in Table I, and the form of melting peaks may be ascribed to the disruption of PVA crystallization with the increase in PSSNa. Indeed, the crystallization of a polymer results from the association of chains into an ordered structure by hydrogen bonds and/or Van der Walls interactions. Such a chain organization occurs during the solvent evaporation process, when the solvent plasticized chains are still mobile enough, before complete freezing of the material. It is driven by the possibility of generation of favorable interactions (with negative enthalpy) in the PVA phase, e.g. when the chains are folded into ordered structures at short, medium, and long-range distance. The introduced PSSNa chains effectively prevent the chain organization into ordered structures, by

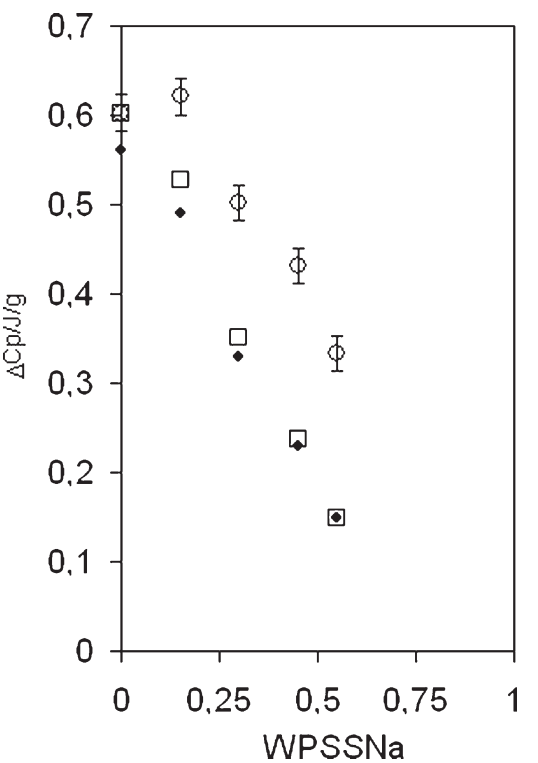

Figure 4 Experimental and calculated heat capacities at T_g, ΔC_P (●), ΔC_{P1} (□) and ΔC_{P2} (○) vs. PSSNa fraction in PVA/PSSNa blends.

perturbing the environment of potential interacting groups.

The interactions inside the studied materials systems using the values of $\Delta Cp_{2(T_g)}$ can be analyzed in the frame of the "strong" - "fragile" concept proposed by Angell.[31] For many glass forming liquid, it was shown that the Arrhenius-like plots of the shear viscosity as a function of the dimensionless temperature T_g/T lead to two different types of materials. An Arrhenius-like law (linear increase in the logarithm of viscosity with T_g/T) sets the upper limit. The glass-forming liquids exhibiting small deviations from this limit are qualified as strong and those showing large deviations are fragile (not in the mechanical sense). The relationship between the behaviors in the liquid and the glassy states with regard to the "strong-fragile" concept is experimentally reflected by the values of $\Delta C_{p(T_g)}$. Indeed, a strong glass-forming liquid will give rise to a glassy structure close to its thermodynamic equilibrium and is characterized by a low value of $\Delta C_{p(T_g)}$ (e.g., 0.1 J/g K). On the contrary, a high value of $\Delta C_{p(T_g)}$ (e.g., 0.4 J/g K) is the signature of a glassy structure far away from its thermodynamical equilibrium state, i.e. that of a fragile glass-forming liquid. Despite the strong-fragile concept is not universal and some exceptions can be found,[31] the major part of glass-forming liquids of organic polymer type seems to follow the general observations. For compositions up to 20% of PSSNa, the values of $\Delta C_{p2(T_g)}$ exhibit the characteristic of fragile system, for higher PSSNa content, the fragile character decreases to lead progressively to a strong material.

It seems that the strong–fragile concept, which was scarcely used to analyze the behavior of polymer blends, may bring valuable information. For instance, as a more strong material, the PVA/PSSNa 55/45 blend must have exponential relaxation features with a Lorentzial relaxation spectrum; the structural dependence of the relaxation time is minimized and linear regime for temperature or pressure perturbations from equilibrium is extended.[31] On the contrary, the more fragile PVA-rich materials would have their relaxation times very state dependent, e.g. the shape of the glass transition observed during reheating would depend strongly on the previous thermal history (because of a precooling, annealing before reheating,...).

Polymer–polymer interactions based on infrared data

To the information obtained from the study of macroscopic parameters in DSC, infrared studies will throw more light on the molecular aspects of the interactions in the polymer systems. Although the miscibility is not directly detected by infrared spectroscopy, a progressive shift in the infrared bands with the blend composition are strong indications of a miscibility. In fact, IR bands are only sensitive to changes around vibrating bonds at very short distance, like those involved in group interactions; without polymer miscibility at the molecular level, the polymer chemical groups would have their environment identical to that in the pure polymer.

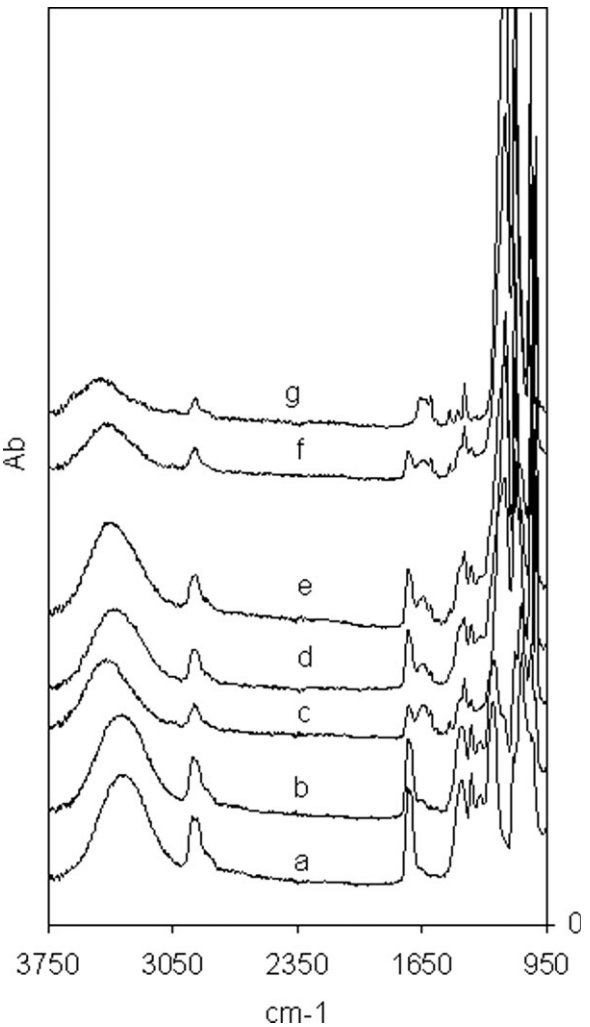

Figure 5 ATR-FTIR spectra of PVA/PSSNa: (a) 100/0, (b) 85/15, (c) 70/30, (d) 55/45, (e) 45/55, (f) 25/75, and (g) 0/100 blends.

The ATR-FTIR spectra obtained for PVA/PSSNa blends at different compositions are shown in Figure 5. Spectral details in the pertinent wavelength ranges for interacting groups are summerized in Table II. The change in the vibration band of several groups as hydroxyl, carbonyl, acetate, phenyl, symmetric and asymmetric sulfonate groups is the result of intermolecular interactions between polymers. These interactions are at the origin of the new arrangement of PVA and PSSNa chains shown by the DSC measurements.

TABLE II
Maximum Wavelength Absorption of Different Groups in the ATR-FTIR Spectra of PVA/PSSNa Blends

PVA/PSSNa	ν_{OH}	$\nu_{C=O}$	ν_{φ}	δ_{CH2}	ν_{COOCH3}	$\nu_{SO3Na\ asym.}$	$\nu_{C\text{-}OH\ crystal.}$	$\nu_{SO3Na\ sym.}$
100 / 0	3332	1734	–	1433	1254	–	1141	–
85 / 15	3335	1731	1647	1430	1247	1198	1141	1042
70 / 30	3370	1731	1647	1426	1237	1191	–	1042
55 / 45	3388	1731	1647	1416	–	1188	–	1042
45 / 55	3409	1731	1647	1416	–	1186	–	1042
25 / 75	3419	1727	1647	1416	–	1185	–	1044
0 / 100	3460	–	1664	1416	–	1188	–	1048

As shown in Figure 6, the band of stretching vibration of O—H (3332 cm^{-1}) within PVA shifts toward higher wavenumbers when the material is progressively enriched in PSSNa whereas the band of carbonyl groups (1734 cm^{-1}) shifts toward lower wave numbers as shown in Figure 7. The band of the stretching vibration of phenyl groups (1664 cm^{-1}), within PSSNa, shifts significantly toward lower wavenumbers.

Moreover, as shown in Figure 8, the deformation band of methylene groups —CH_2— shifts from 1433 cm^{-1} to lower wavenumbers as well as the stretching band of acetate groups (1254 cm^{-1}) decreases by 17 cm^{-1}. It can also be seen that the band of stretching vibration of asymmetric sulfonate groups (1188 cm^{-1}) shifts slightly toward lower wavenumbers and then it increases, whereas that of symmetric sulfonate groups (—SO_3^-) shifs from 1048 cm^{-1} to lower wevenumbers as shown in Figure 9. This behavior may be interpreted as the consequence of the change in intermolecular interactions in the surrounding of groups.

The broadband centered at 3332 cm^{-1} in the PVA spectrum is considered as the result of the stretching

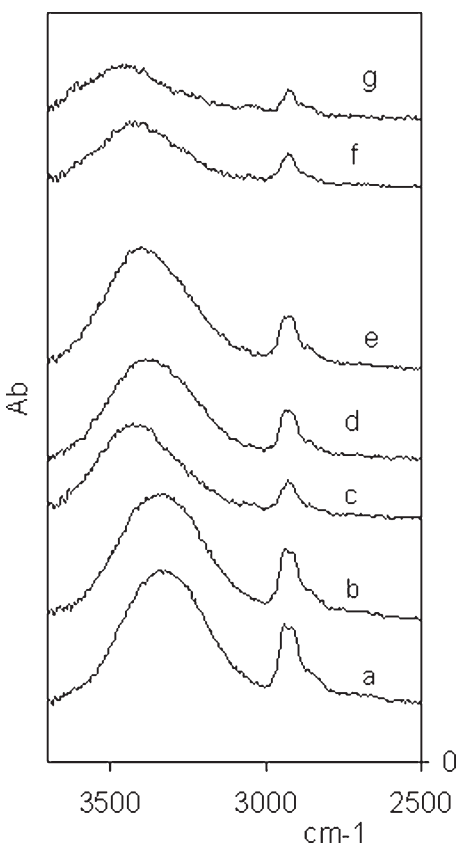

Figure 6 Stretching vibration peaks of hydroxyl groups within PVA/PSSNa: (a) 100/0, (b) 85/15, (c) 70/30, (d) 55/45, (e) 45/55, (f) 25/75, and (g) 0/100 blends.

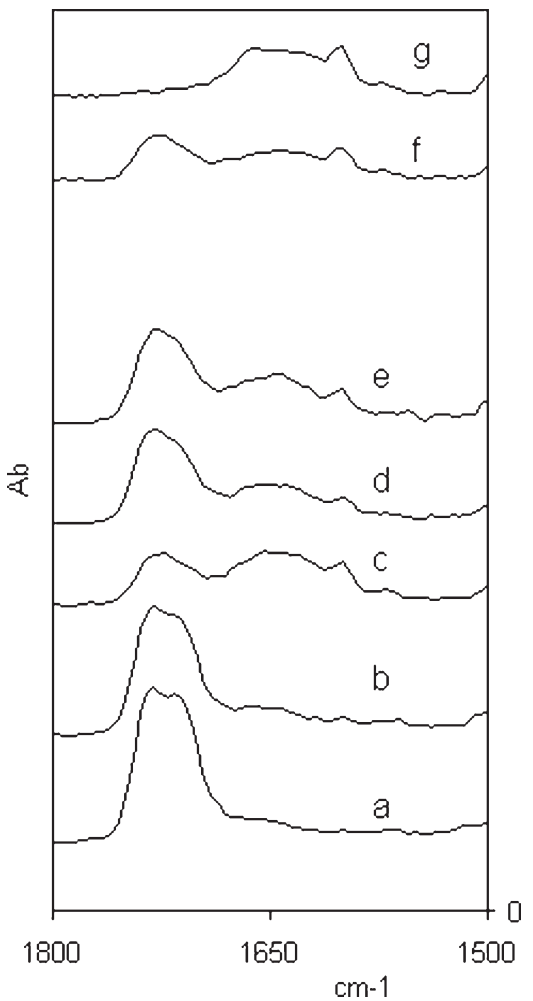

Figure 7 Stretching vibration peaks of carbonyl groups (1734 cm^{-1}) and phenyl (1664 cm^{-1}) within PVA/PSSNa: (a) 100/0, (b) 85/15, (c) 70/30, (d) 55/45, (e) 45/55, (f) 25/75, and (g) 0/100 blends.

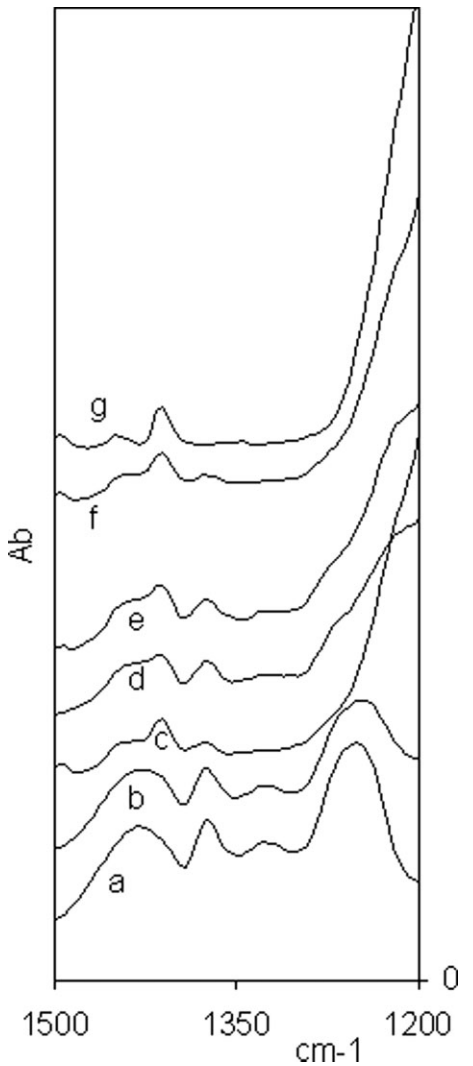

Figure 8 Stretching vibration peaks of acetate groups (1254 cm^{-1}) and deformation peaks of —CH_2— groups (1433 cm^{-1}) within PVA/PSSNa: (a) 100/0, (b) 85/15, (c) 70/30, (d) 55/45, (e) 45/55, (f) 25/75, and (g) 0/100 blends.

vibration of different hydrogen bonds of OH groups. The contribution of a large number of strong intrachain hydrogen bond[9,32] between the OH along the PVA chains in the zig-zag configuration is probably responsible for the exceptional low wavenumber value compared with that of an isolated (not bound) OH group.[33] The shift in the OH— vibration wave numbers to higher values can be interpreted as a consequence of the decrease in the number of (strong) intrachain hydrogen bonds in favor of interchain ones. Although, there is a positive driving force for such strong interactions, the presence of an increasing amount of PSSNa hinders more and more the organization of PVA chain into crystallites. This interpretation is supported by the progressive disappearance of the peak at 1141 cm^{-1}, as shown in Figure 9, whose intensity is related to the crystallinity degree[6,8,20,28] and by the above DSC data.

Zundel[34,35] attributed the band at 3460 cm^{-1} in the hydrated PSSNa spectrum to the stretching vibration of hydroxyl groups in hydration water molecules. He showed that the OH wavenumber depends on the nature of polyions, the nature of counterion, and the degree of hydration. He suggested that the water molecules are attached with their lone pairs to the cations (Na^+) and are bound *via* hydrogen bonds to the anions (—SO_3^-), and the polarization of the OH groups of the water molecules by the electrostatic field of the cation strengthens the hydrogen bond.[35]

By a similar mechanism, the OH stretching vibration band would shift toward lower wave numbers when the hydroxyl group is involved in the interactions with the PSSNa sulfonate. However, the shift toward higher wavenumbers, observed for PVA hydroxyl when it is blended with an increasing amount of PSSNa, is a relative shift from a position that corresponds to the strongest hydrogen bond in PVA, i.e. that in the crystalline phase. The crossinteractions between hydroxyl groups on the PVA chains

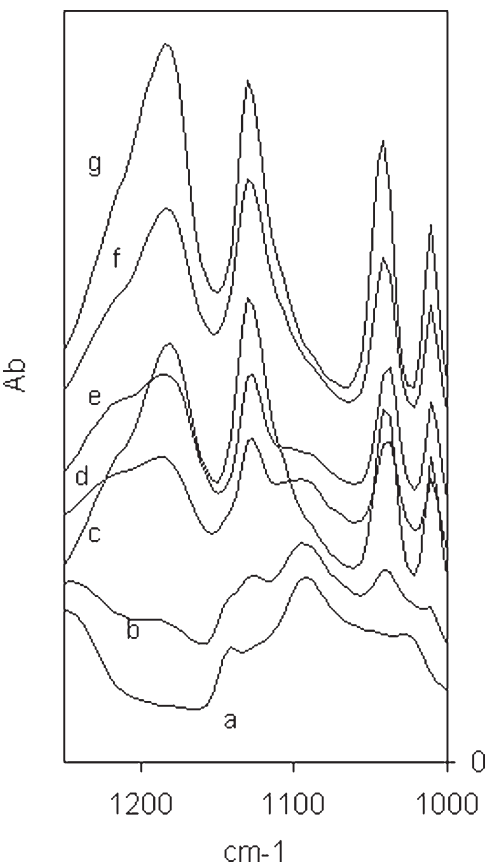

Figure 9 Stretching vibration peaks of asymmetric (1188 cm^{-1}) and symmetric (1048 cm^{-1}) sulfonate groups and —C—O bond (1097 cm^{-1}) within PVA/PSSNa: (a) 100/0, (b) 85/15, (c) 70/30, (d) 55/45, (e) 45/55, (f) 25/75, and (g) 0/100 blends.

and the sulfonate groups on the PSSNa chains in the blend make the reorganization of the PVA chains into crystallites (in which the hydrogen bond is the strongest) very difficult. The larger the sulfonate number in the solid materials, the weaker the average strength of the hydrogen bond per OH group (i.e. higher OH wavenumber), as more OH is bound in larger proportion with the sodium sulfonate at the expense of that in PVA crystallites. The reinforcement of the hydrogen bonds between OH and SO_3^- due to the interactions of the Na^+ cation with the OH dipole would enable the hindering of PVA crystallization by PSSNa and make the two polymers miscible. It should be noted that the fully hydrolyzed PVA has much poorer compatibility with PSSNa. Apparently, the hydrogen bonds between OH and SO_3^- are not energetic enough compared with those that would be created in the fully hydrolyzed PVA, which is endowed with stronger crystallization potential than the partially hydrolyzed PVA used in this study.

Based on the data reported in the literature, we assign the 1254 cm^{-1} band to the stretching vibration of acetate groups (—OC—O—CH_3) in PVA, and the 1188 cm^{-1} band to asymmetric stretching vibration of the —SO_3^- ions.[35,36] The shift in —C—O— stretching vibration bands toward smaller wave numbers (Fig. 8) indicates other interactions between PVA and PSSNa. We suggest that the oxygen atom in the amorphous —C—O groups may form dipole–ion interactions with sodium counterion of the sulfonate groups (—$SO_3^-Na^+$). The interactions between PVA and the —$SO_3^-Na^+$ group are also reflected by the slight shift of symmetric vibration bands of the —SO_3^- to lower wave numbers (Fig. 9). Sodium cations seemed to be involved in electrostatic interactions,[1] which altered the vibrations of the symmetrically paired sulfonate groups. Moreover, the shift of vibration bands of phenyl groups, by 17 cm^{-1}, toward lower wave numbers constitutes another sign of PVA and PSSNa intermolecular interactions. These groups are well known to induce Van Der Walls interactions due to its plane and polarizable structure.[37]

Blend-film morphology by scanning electron microscopy

Films obtained from compatible polymers often show unique continuous phase whereas those obtained from uncompatible or partially compatible polymers lead to different coarse or fine phases due to the phase separation. Figure 10 presented the cross-section micrographs, by scanning electron microscopy (SEM), of PVA/PSSNa 100/0, 70/30, 45/5,5 and 25/75 at two magnifications.

From the analysis of different SEM micrographs, it seems that the PVA/PSSNa films are totally homogeneous. The small bright points that appear in pure PVA film as well as in PVA/PSSNA blend films can be assigned to the impurity traces. It should be noted that heterogeneous blend films were observed with PVA of highest hydrolysis degree. The hydrolysis

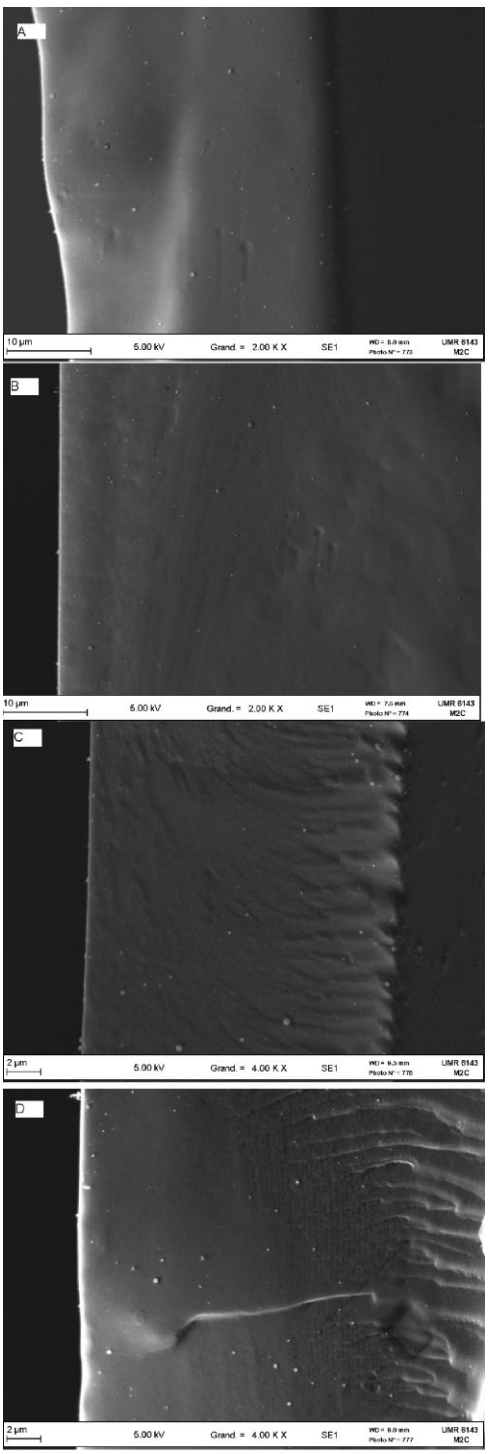

Figure 10 Cross-sectional SEM micrographs of PVA/PSSNa blends (a) PVA 100% with 2KX, (b) PVA/PSSNa 70/30 with 2KX, (c) PVA/PSSNa 45/55 with 4KX, and (d) PVA/PSSNa 25/75 with 4KX. The arrows show the top surface of membrane.

degree seems to be the key of PVA– PSSNa compatibility. The PVA–PSSNa compatibility would be driven by the decrease in the hydrolysis degree of PVA.[38] The higher the number of distributed acetate groups that remain randomly on the chains after incomplete hydrolysis, the weaker the interactions among OH groups, and the lower the crystallinity.

CONCLUSIONS

The investigation of PVA/PSSNa blends by DSC, ATR-FTIR, and SEM showed the compatibility of these polymers in solid state. This compatibility is promoted by specific interactions like hydrogen bonds and dipole–ion interactions between hydroxyl groups of PVA, on the one hand, and, the sulfonate and pheny groups of PSSNa, on the other hand.

The calorimetric data show that for compositions up to 20% of PSSNa, the intermolecular interactions between PVA and PSSNa segments are very weak to overcome completely the intramolecular interactions between hydroxyl groups along PVA chains, whereas for higher content of PSSNa, the establishment of strong interactions between polymer segments induces the inhibition of the PVA crystallization, in the one hand, and the PVA and PSSNa compatibility, in the other hand. Such results are confirmed, in the one hand, by the FTIR data: the shift of the band of stretching vibration of O—H, phenyl, acetate, and sulfonate groups, and in the other hand, by the SEM observations: polymer's mixtures lead to unique homogeneous phase.

We thank the France goverment (SCAC Amprun project, Nouakchott, Mauritania) for the financial support that help us to achieve this work.

References

1. Hara, M.; Eisenberg, A. Macromolecules 1987, 20, 2160.
2. Sonja, K. Polymer Handbook; 3rd ed, Chap. VI/347. John Wiley & Sons: New York, 1989.
3. Perrau, M. B.; Iliopoulos, I.; Andelbert, R. Polymer 1989, 30, 2112.
4. Nishi, T.; Kwei, T. K. Polymer 1975, 16, 285.
5. Juana, R.; Cortazar, M. Macromolecules 1993, 26, 1170.
6. Krimm, S. Forsch Bd. 2, 1960, 51.
7. Shibayama, M.; Yamamoto, T.; Xiao, C. F.; Sakurai, S.; Hayami, A.; Nomura, S. Polymer 1991, 32, 1010.
8. Miya, M.; Iwamoto, R. J Polym Sci Polym Phys 1984, 22, 1149.
9. Daniliuc, L.; Kesel, C. D.; David, C. Eur Polym J 1992, 28, 1365.
10. Paul, D. R.; Barlow, J. W. Polymer 1985, 25, 487.
11. Metayer, M.; Mbareck, C. O. React Funct Polym 1997, 33, 311.
12. Ping, Z. H.; Nguyen, Q. T.; Néel, J. J Makromol Chem 1990, 191, 185.
13. Staszewska, D.; Bohdanecky, M. Eur Polym J 1981, 17, 245.
14. Zhang, X.; Takegoshi, K.; Hikichi, K. Polymer 1992, 33, 718.
15. Painter, P. C.; Park, Y.; Coleman, M. M. Macromolecules 1989, 22, 570.
16. Mbareck, C. O.; Metayer, M.; Langevin, D.; Roudesly., S. J Appl Polym Sci 1996, 62, 161.
17. Goh, S. H.; Siow, K. S.; Lee, S. Y. Eur Polym J 1991, 27, 921.
18. Coleman, M. M.; Skrovanek, D. J.; Hu, J.; Painter, P. C. Macromolecules 1988, 21, 59.
19. Finch, C. A. Polyvinyl Alcohol.John Wiley & Sons: New York, 1973.
20. Kenny, J. F.; Willcockson, G. W. J Polym Sci Part A Polym Chem 1966, 4, 679.
21. Nishio, Y.; Haratani, T.; Takahasini, T.; Manley, J. Macromolecules 1989, 22, 2547.
22. Peppas, N.; Merrelli, E. W. J Appl Polym Sci 1976, 20, 1457.
23. Zhong, Z.; Guo, Q. Polymer 1998, 39, 517.
24. Sahu, A. K. J Memb Sci 2008, 319, 298.
25. Kang, M. S. J Memb Sci 2005, 247, 127.
26. Sahu, A. K. J Electrochem Soc 2008, 155, B686.
27. Lau, C.; Mi, Y. Polymer 2002, 43, 823.
28. Mallapragada, S. K.; Peppas, N. A. J Polym Sci Polym Phys 1996, 34, 1339.
29. Nishi, T.; Wang, T. T. Macromolecules 1975, 8, 909.
30. Imken, R. L.; Paul, D. R.; Barlow, J. W. Polym Eng Sci 1976, 16, 593.
31. Angell, C. A. J Noncryst Solids 1991, 131, 13.
32. Caver, C. D. Desk Book of Infrared Spectra, 2nd ed.; Coblentz Soc. Inc.: Kirkwood, MO, 1986, p 35–239.
33. Nguyen, Q. T.; Favre, E.; Ping, Z. H.; Néel, J. J Memb Sci 1996, 113, 137.
34. Zundel, G. Hydration and Intermolecular Interactions; Acadamic Press: New York and London, 1969.
35. Zundel, G. J Memb Sci 1982, 11, 249.
36. Bellamy, L. J. The Infra-Red Spectra of Complex Molecules; Champan and Hall: London, 1975.
37. Ma, J.; Cui, P.; Zhao, L.; Huang, R. Eur Polym J 2002, 38, 627.
38. David, M. O.; Nguyen, T. Q. Eur Polym J 1994, 30, 1013.